Water Confinement in Small Polycyclic Aromatic Hydrocarbons

Alon Zamir,[1] Estefania R. Molina,[1] Musahid Ahmed,[2] Tamar Stein[1]*

[1] Fritz Haber Research Center for Molecular Dynamics, Hebrew University of Jerusalem, Jerusalem 9190401, Israel

[2] Chemical Sciences Division, Lawrence Berkeley National Laboratory, Berkeley, California 94720, USA

*Corresponding author: tamar.stein@mail.huji.ac.il

Abstract

The confinement of water molecules is vital in fields from biology to nanotechnology. The conditions allowing confinement in small finite polycyclic aromatic hydrocarbons (PAHs) are unclear, yet they are crucial for understanding confinement in larger systems. Here, we report a computational study of water cluster confinement within PAHs dimers. Our results serve as a model for larger carbon allotropes and understanding molecular interactions in confined systems. We identified size and structural motifs allowing confinement and demonstrated the motifs in various PAHs systems. We show that optimal OH···π interactions between water clusters and the PAH dimer permit optimal confinement to occur. However, the lack of such interactions leads to the formation of CH···O interactions, resulting in less ideal confinement. Confinement of layered clusters is also possible, provided that the optimal OH···π interactions are conserved.

The ability to confine water in nonpolar pores is of significant interest in various fields, including biology, nanotechnology, and nanofluids.[1] The presence of water in nonpolar cavities near protein active sites directly enables many biological processes.[2] Interestingly, water flows through such hydrophobic pores or cavities at the nanoscale display markedly lower wall friction and a higher flow rate compared to the macroscopic level. This nanoscale flow, such as water confinement in a carbon nanotube (CNT), has great potential for applications in many areas.[3-5] For example, CNTs are of interest in gas storage containers,[6] water purification, and hydrogen production.[7]

The interaction between graphene allotropes with water, including graphite, CNTs, and fullerene is widely studied using both computational and experimental methods. Computationally, water molecule adsorption to the carbon surface was modeled using *ab-initio* methods and density functional theory (DFT) calculations.[8-12] Water confinement within carbon nanotubes was also studied computationally with DFT methods, with the conclusion that water molecules cluster near the inner CNT wall due to favorable OH$\cdots\pi$ interactions between the water and the CNT. [13] Interestingly, molecular dynamic simulations revealed the importance of the orientation of the water molecules; an orientation that enables OH$\cdots\pi$ interactions is dominant for both adsorption upon a surface and for confinement.[12, 14-17]

Experimentally, the unique nature of water hydrogen bonding inside CNTs was demonstrated by vibrational spectroscopy, showing intra-ring and inter-ring hydrogen bonds.[17] In addition to the effects of confinement on the hydrogen bonding, the results of confinement on water diffusion and charge migration within an aqueous medium were also studied. [18] Finally, both experimental [19] and theoretical [20] work indicate that confinement of water in tiny cavities (up to 1 nm in diameter) results in clusters arranged in either a monolayer or bilayer. [21, 22] The confined water displays unusual properties which differ significantly from bulk water due to a modified hydrogen bond network.[23, 24]

Overall, the computational work, particularly the *ab-initio* calculations describing molecular-level interactions, emphasizes the importance of relative orientations between carbon surfaces and water molecules on the binding energies (BE).[25-27] Notably, much of this previous works used the polycyclic aromatic hydrocarbon (PAH) which can serve as model systems to graphene and CNT, to determine their interaction with water.[14, 28, 29] In one example, Hirunsit *et al.* modeled the confinement of two to four water molecules within a benzene or naphthalene dimer [30]. They determined that a water cluster with up to four molecules cannot be confined within the naphthalene dimer, which served as a model for graphite sheets. However, artificial constraints that were imposed enabled the confinement. Without these artificial constraints, water molecules moved to the side of the naphthalene, where they formed CH$\cdots$O interactions. In related work, Molina *et al.* studied an anthracene dimer complexed to water clusters that

contained up to four water molecules.[29] In the case of one to three water molecules, confinement of water within the dimer was not observed, and the optimal structures had water in a side orientation relative to the anthracene. With four water molecules, confinement was observed when the anthracene dimers were in a cross configuration, which enabled optimal OH$\cdots\pi$ interactions to form. Because anthracene and naphthalene are three and two linearly fused benzene rings, respectively, the additional aromatic ring is important for determining whether a PAH can confine water clusters and the size of the cluster that can be confined. Molina *et al.* also compared complexes of water and anthracene dimers, demonstrating that water tends to remain self-clustered. Among the possible structural isomers tested, only in the case of four water molecules inside the anthracene dimer in a cross-configuration confinement was observed.

In this study, we explored the conditions enabling water confinement inside small PAH systems. Consequently, we focused only on isomers that showed confinement of water molecules within the PAHs without artificial constraints. We first compared different PAH dimers confining clusters of four waters because optimal OH$\cdots\pi$ interactions are demonstrated by Molina *et al.* to achieve four-water confinement in the anthracene dimer. We next study the effect of reducing the number of waters on the confinement; as the infrastructure for optimal OH$\cdots\pi$ interactions is not attainable on lower amount of water molecules. We additionally report the interaction between water clusters containing five and six water molecules with various PAHsof different sizes and structures and layered water clusters containing 8 and 12 water molecules with anthracene. We reveal the size and structural motifs enabling confinement at the molecular level, which is crucial for understanding confinement in larger systems such as a CNT.

To quantify the confinement, we measured BEs of the complexed water-PAH dimer systems to determine the energetic favorability of confinement. Additionally, we examined the tilting angle between the confining dimers because interaction within the dimer varies with the displacement. Water molecules could thus escape the confinement more freely due to the tilting angle.

We performed density functional theory (DFT) calculations using the $\omega B97X-V$ functional, which accounted for van der Waals interactions and was thus suitable to study cluster systems.[31] Structures were optimized using the cc-pVTZ basis set[32] followed by frequency calculations to verify that they are minima on the potential energy surfaces (PES). To calculate BEs, we performed single-point using $\omega B97X-V$ with the aug-cc-PVTZ basis set on the relaxed structures.[33] The BEs were determined as follows: $BE = E_{complex} - 2 \cdot E_{PAH} - n \cdot E_{water}$. All structures presented exhibited negative BEs and as we increased the size of the water clusters, the BEs increased significantly. For comparison, we divided the BEs by the number of water molecules to yield the absolute values of the normalized BE (*n*BE). All calculations were performed with the Q-Chem 5.4 software package.[34] To study possible confinement, we examined dimer structures with confined water then performed structural optimization from that starting point. We concluded that confinement was possible in cases where water stayed within the dimer after optimization.

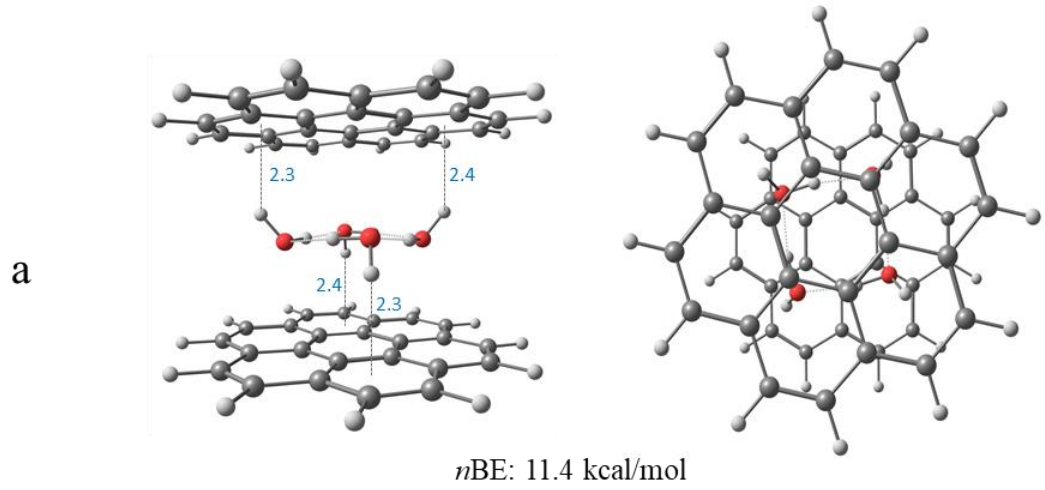

Figure 1: Side (left panel) and top view (right panel) of clusters of four waters confined within two coronenes (a), two anthanthrenes (b), and two fluorenes (c). All reported bond lengths are in Å. The blue numbers indicate the OH···π bond lengths, and the green numbers indicate the CH···O bond lengths.

We optimized dimer structures of coronene, anthanthrene, and fluorene with four water molecules (Figure 1). Similar to anthracene reported by Molina *et al.*[29] coronene (Figure 1a) and anthanthrene (Figure 1b) have large planar surfaces that can ideally confine the clusters within the dimer. The confinement is achieved by the formation of optimal OH···π interactions between the non-contiguous hydrogens and π clouds of the acenes. Interestingly, cross (Figure 1b) and parallel (Figure S1a) configurations enabled confinement in anthanthrene because stabilizing interactions were possible for each configuration. Both coronene and anthanthrene exhibited similar *n*BEs of 11.4 kcal/mol and 11.1 kcal/mol, respectively. Ideal confinement of four water molecules was also observed for a pyrene dimer (Figure S1c).

We also found possible confinement for fluorene (Figure 1c). Due to the non-linearly fused-ring structure and its non-planar hydrogens, we observed additional stabilizing CH···O interactions between oxygen in two of the water molecules and hydrogens in the bay region (see figure S2) of the acenes. These interactions resulted in a slight tilting angle of 10.3˚. Despite the non-optimal confinement, additional stabilization was obtained via the CH···O interactions. In this case, the close CH···O interactions (2.3 Å between H and O) resulted in an *n*BE of 12.3 kcal/mol, the greatest value among the molecules we examined. For phenanthrene (Figure S1b), the additional CH···O interactions resulted in a tilting angle of 11.2° and a favorable *n*BE of 11.3 kcal/mol, slightly lower than the 12.3 kcal/mol observed for fluorene.

The confined water clusters do not show significant structural differences with their corresponding isolated water cluster. The small alterations in the confined cluster is a direct result of OH···π and CH···O interactions. Figure S3 presents illustrative examples of the overlap of isolated and confined clusters, and table S1 provides the corresponding root-mean-square deviationbetween the structures.

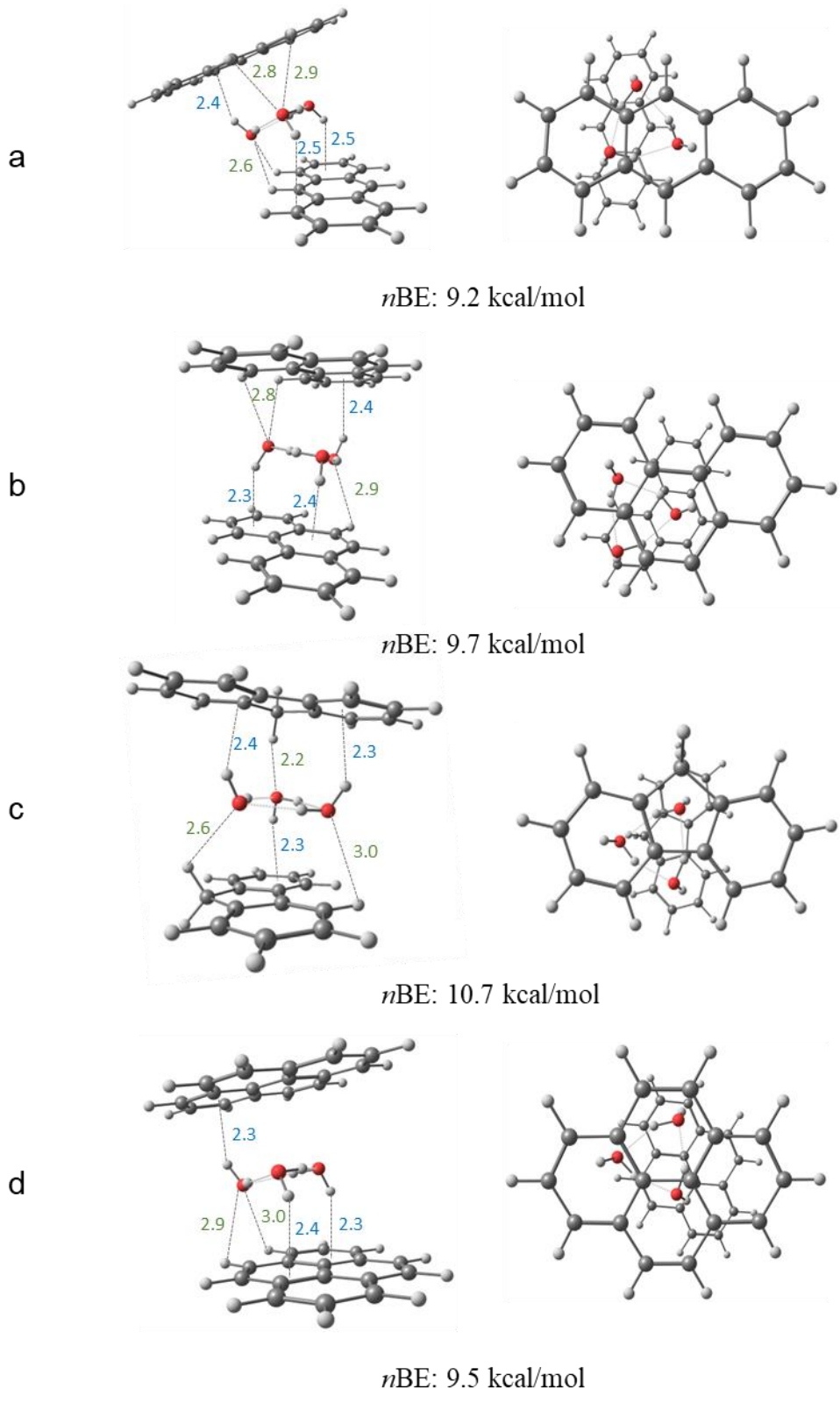

Figure 2: Side (left panel) and top view (right panel) of clusters of three waters confined within anthracenes (a), phenanthrenes (b), fluorenes (c), and pyrenes (d) from the side view (left panel) and top view (right panel). All reported bond lengths are in Å. The blue numbers indicate the OH···π bond lengths, and the green numbers indicate the CH···O bond lengths.

We next analyzed the confinement of water clusters containing three water molecules within anthracene, phenanthrene, fluorene, and pyrene (Figure 2). In this case, we did not expect ideal confinement of the water cluster because two contiguous hydrogens pointed upward and one pointed downward, leading to a non-symmetrical structure and a preference for one side. This is well demonstrated in the case of anthracene dimer (Figure 2a). Upon optimization, the water cluster is moving to form CH···O interactions. The interactions resulted in the movement of the top anthracene and a large tilting angle of 18.5˚. The confinement was weakened severely, and the non-ideal interactions are demonstrated by the low *n*BE of 9.2 kcal/mol.

We examined the confinement of the water cluster inside phenanthrene (Figure 2b) and fluorene (Figure 2c). The PAHs are similar in length and shape; however, fluorene is not aromatic due to the presence of a saturated methylene group. The molecules showed tilting angles of 6.7˚(phenanthrene) and 9.1˚(fluorene) (Figure 2). In the case of phenanthrene (Figure 2b), two hydrogens of the water molecule pointed downward and interacted with the bottom PAH via OH··· π interactions. Interaction with the top PAH occurred via one OH···π interaction and additional CH···O bonds in the bay region (length 2.8Å). Due to the position of the oxygen involved in the formation of the CH···O bond, effective confinement was possible. For fluorene (Figure 2c), confinement was enabled by strong CH···O interactions due to the small distances between the hydrogen atoms in the middle ring and the oxygen atoms in the water clusters. The strong CH···O interactions resulted in a large *n*BE of 10.7 kcal/mol compared to 9.7 kcal/mol for phenanthrene. We concluded that the difference between phenanthrene and fluorene validated the importance of PAH geometry in addition to water cluster size and geometry.

Pyrene, although similar to phenanthrene in length, did not form additional CH···O interactions due to lack of the bay region. This lack of interaction resulted in an *n*BE of 9.5 kcal/mol (Figure 2d). Overall, the structures confining three water molecules had lower *n*BEs than those confining four water molecules due to the lack of additional stabilizing OH···π interaction.

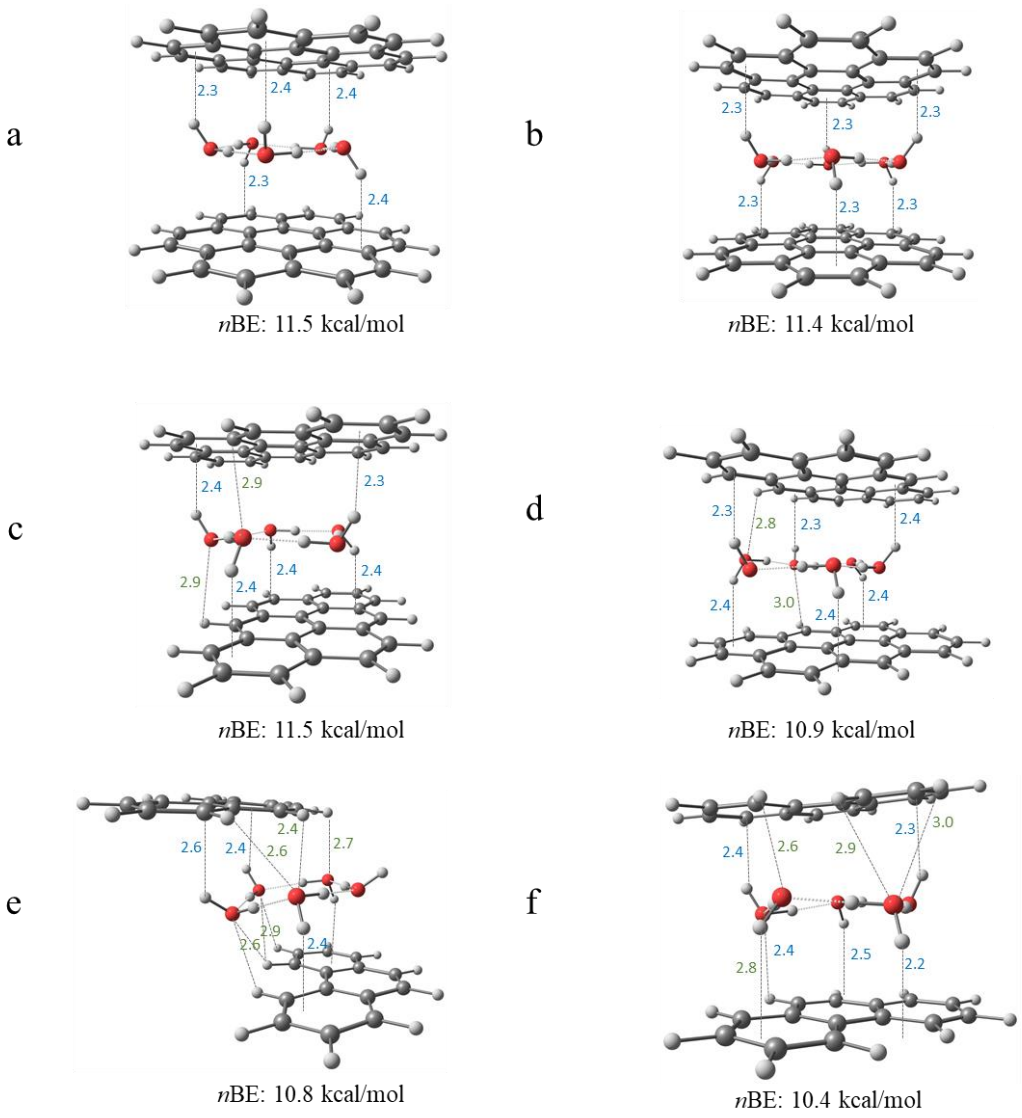

Figure 3: Side views of clusters of five and six waters confined within coronenes (a, b), anthanthrenes (c, d), and five water molecules with two conformers of phenanthrenes (e, f). All reported bond lengths are in Å. The blue numbers indicate the OH···π bond lengths, and the green numbers indicate the CH···O bond lengths. Top views are included in Figure S4.

Next, we demonstrated the confinement of five and six water molecules (Figure 3). Coronene (Figures 3a, 3b) was large enough to confine clusters of five and six water molecules optimally. These water cluster-coronene dimers did not exhibit tilting angles, and their optimal confinement was evidenced by large *n*BEs of 11.5 kcal/mol and 11.4 kcal/mol for clusters of five and six waters, respectively. Similarly, anthanthrene was large enough to contain a five-ringed water cluster with optimal confinement (Figure 3c). Again, we observed no tilting angle, and the calculated *n*BE was 11.5 kcal/mol, indicating strong confinement. For the confinement of a cluster of six waters (Figure 3d), the relative sizes of the clusters and the dimer resulted in the partial protrusion of water molecules outside the dimer, resulting in less optimal OH··· π interactions and a lower *n*BE of 10.9 kcal/mol.

We found that a cluster with five water molecules could form within the phenanthrene dimer (for optimized structure, see Figure 3e). Due to the small size of the PAH, the formation of optimal OH$\cdots$ π interactions was prohibited, resulting in a shift in one ring to enable interactions with CH$\cdots$O. The resulting structure did not confine the water, and the *n*BE was 10.8 kcal/mol. We identified a second energy minimum (Figure 3f) where the cluster was partially confined. However, due to the size of the PAH, some of the water molecules protruded, resulting in CH$\cdots$O interaction. The structure resulted in a tilting angle of 11.2˚ and an *n*BE of 10.4 kcal/mol, which was smaller than the *n*BE value observed in previous cases. We observed similar trends for six waters confined within the phenanthrene dimer (Figure S4b).

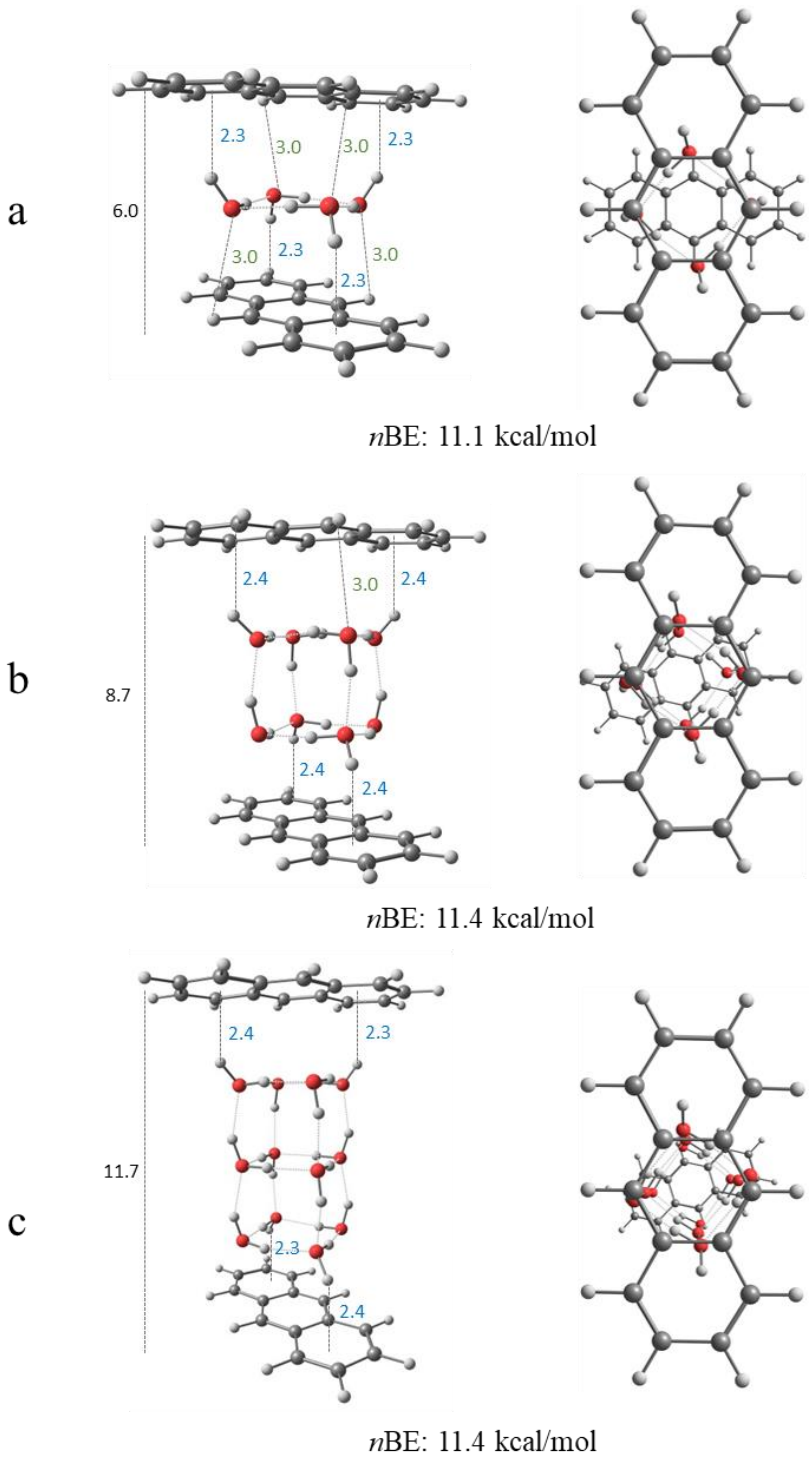

Figure 4: Side (left panel) and top view (right panel) of clusters of four (a), eight (b), and twelve (c) waters confined within anthracene dimers from the side view (left panel) and top view (right panel). All reported bond lengths are in Å. The blue numbers indicate the OH···π bond lengths, the green numbers indicate the CH···O bond lengths, and the black number indicates the overall distance between the anthracenes.

As mentioned, confined water molecules between graphene sheets may arrange as a monolayer to a bilayer with a distance of 1 nm between sheets. We demonstrated the confinement of eight and twelve water molecules within anthracene, resulting in two and three layers of four water molecules (Figures 4b and 4c, respectively). We observed that the bilayer was optimal at a distance of 0.87 nm between layers, whereas three water layers were optimal at a distance of 1.14 nm between layers. Like graphene, it was feasible to confine additional water molecules by arranging the layers to preserve the ideal OH···π interactions. Our four-water cluster confined within the dimer showed an *n*BE of 11.1 kcal/mol, whereas the *n*BEs of eight and twelve water clusters were 11.4 kcal/mol.

In conclusion, there were key similarities between water confinement within PAHs and low-dimensional carbon surfaces because both relate to underlying intermolecular interactions between polar water molecules and the non-polar aromatic surfaces. Here, we demonstrated the key role of the molecular orientation in enabling stabilizing OH···π interactions. Nonetheless, there were noticeable differences. For low-dimensional carbon surfaces such as graphene, discrete PAH dimers benefited from CH···O interactions. In contrast, in graphene-like materials, these interactions were negligible because the majority of the interactions relied on OH···π. Although the tilting angle reduced the optimal OH···π interactions between the water and the dimers, these interactions were compensated by other CH···O interactions, as we demonstrated by our quantitative *n*BE values. While the BE increased with the addition of water molecules, the *n*BE value was consistent in studied systems, with values ranging between 9.2-12.3 kcal/mol.

From our results, we can generalize that ideal confinement due to OH···π interactions results in *n*BE values of approximately 11.5 kcal/mol, with a required interaction distance of 2.3-2.4 Å. The size of a water cluster and its relative proportion to a dimer directly affects interactions and whether confinement will occur. As we demonstrated for anthracene, it is possible to confine two or three water layers if the optimal OH···π interactions are preserved. Our results will guide future experiments using vibrational spectroscopy, as demonstrated recently for pure water clusters [35-37], to probe the stability and structure of PAH water clusters. These results will provide insight into the confinement of water. The ideas of confinement we have developed in this work could enhance our understanding of anthracene cluster interactions with water ice [38] and in anthracene dimer exciplex formation in solution,[39] both of which have relevance in a wide variety of sub-disciplines.

Acknowledgments:

TS, AZ, and ERM were supported by The Israel Science Foundation under Grant No. 1941/20. AZ was supported by The Harvery M.Krueger Family Center for Nanoscience and Nanotechnology, the Hebrew University of Jerusalem.MA was supported by the Director, Office of Science, Office of Basic Energy Sciences, of the US Department of Energy under Contract No. DE-AC02-05CH11231 through the Gas Phase Chemical Physics Program, Chemical Sciences Division.

1. Giovambattista, N., P.J. Rossky, and P.G. Debenedetti, *Computational Studies of Pressure, Temperature, and Surface Effects on the Structure and Thermodynamics of Confined Water.* Annual Review of Physical Chemistry, 2012. **63**(1): p. 179-200.
2. Bellissent-Funel, M.-C., et al., *Water Determines the Structure and Dynamics of Proteins.* Chemical Reviews, 2016. **116**(13): p. 7673-7697.
3. Guo, Y., et al., *Co2P–CoN double active centers confined in N-doped carbon nanotube: heterostructural engineering for trifunctional catalysis toward HER, ORR, OER, and Zn–air batteries driven water splitting.* Advanced Functional Materials, 2018. **28**(51): p. 1805641.
4. Marbach, S. and L. Bocquet, *Osmosis, from molecular insights to large-scale applications.* Chemical Society Reviews, 2019. **48**(11): p. 3102-3144.
5. Chin, H.-T., et al., *Ferroelectric 2D ice under graphene confinement.* Nature communications, 2021. **12**(1): p. 1-7.
6. Dillon, A.C., et al., *Storage of hydrogen in single-walled carbon nanotubes.* Nature, 1997. **386**(6623): p. 377-379.
7. Frappa, M., et al., *A few-layer graphene for advanced composite PVDF membranes dedicated to water desalination: A comparative study.* Nanoscale Advances, 2020. **2**(10): p. 4728-4739.
8. Kysilka, J., et al., *Accurate Description of Argon and Water Adsorption on Surfaces of Graphene-Based Carbon Allotropes.* The Journal of Physical Chemistry A, 2011. **115**(41): p. 11387-11393.
9. Freitas, R.R.Q., et al., *DFT Studies of the Interactions of a Graphene Layer with Small Water Aggregates.* The Journal of Physical Chemistry A, 2011. **115**(44): p. 12348-12356.
10. Feller, D. and K.D. Jordan, *Estimating the Strength of the Water/Single-Layer Graphite Interaction.* The Journal of Physical Chemistry A, 2000. **104**(44): p. 9971-9975.
11. Feller, D., *Strength of the Benzene−Water Hydrogen Bond.* The Journal of Physical Chemistry A, 1999. **103**(38): p. 7558-7561.
12. Pertsin, A. and M. Grunze, *Water−Graphite Interaction and Behavior of Water Near the Graphite Surface.* The Journal of Physical Chemistry B, 2004. **108**(4): p. 1357-1364.
13. Tripathy, M.K., D.K. Mahawar, and K.R.S. Chandrakumar, *Effect of nano-confinement on the structure and properties of water clusters: An ab initio study.* Journal of Chemical Sciences, 2019. **132**(1): p. 7.

14. Wu, Y. and N. Aluru, *Graphitic carbon–water nonbonded interaction parameters.* The Journal of Physical Chemistry B, 2013. **117**(29): p. 8802-8813.
15. Ayappa, K.G., *Enhancing the Dynamics of Water Confined between Graphene Oxide Surfaces with Janus Interfaces: A Molecular Dynamics Study.* The journal of physical chemistry. B, 2019. **123**(13): p. 2978-2993.
16. Laage, D. and W.H. Thompson, *Reorientation dynamics of nanoconfined water: Power-law decay, hydrogen-bond jumps, and test of a two-state model.* The Journal of chemical physics, 2012. **136**(4): p. 044513.
17. Byl, O., et al., *Unusual Hydrogen Bonding in Water-Filled Carbon Nanotubes.* Journal of the American Chemical Society, 2006. **128**(37): p. 12090-12097.
18. Muñoz-Santiburcio, D. and D. Marx, *Confinement-Controlled Aqueous Chemistry within Nanometric Slit Pores.* Chemical Reviews, 2021. **121**(11): p. 6293-6320.
19. Bampoulis, P., et al., *Hydrophobic ice confined between graphene and MoS2.* The Journal of Physical Chemistry C, 2016. **120**(47): p. 27079-27084.
20. Koga, K., X.C. Zeng, and H. Tanaka, *Freezing of confined water: A bilayer ice phase in hydrophobic nanopores.* Physical review letters, 1997. **79**(26): p. 5262.
21. Cicero, G., et al., *Water confined in nanotubes and between graphene sheets: A first principle study.* Journal of the American Chemical Society, 2008. **130**(6): p. 1871-1878.
22. Eslami, H. and N. Heydari, *Hydrogen bonding in water nanoconfined between graphene surfaces: a molecular dynamics simulation study.* Journal of nanoparticle research, 2014. **16**(1): p. 1-10.
23. Li, Q., et al., *Two-dimensional material confined water.* Accounts of chemical research, 2015. **48**(1): p. 119-127.
24. Park, H.G. and Y. Jung, *Carbon nanofluidics of rapid water transport for energy applications.* Chemical Society Reviews, 2014. **43**(2): p. 565-576.
25. Tripathy, M.K., D.K. Mahawar, and K. Chandrakumar, *Effect of nano-confinement on the structure and properties of water clusters: An ab initio study.* Journal of Chemical Sciences, 2020. **132**(1): p. 1-11.
26. McKenzie, S. and H.C. Kang, *Squeezing water clusters between graphene sheets: energetics, structure, and intermolecular interactions.* Physical Chemistry Chemical Physics, 2014. **16**(47): p. 26004-26015.
27. Rubes, M., et al., *Structure and stability of the water− graphite complexes.* The Journal of Physical Chemistry C, 2009. **113**(19): p. 8412-8419.
28. Xu, B., et al., *Probing solvation and reactivity in ionized polycyclic aromatic hydrocarbon–water clusters with photoionization mass spectrometry and electronic structure calculations.* Faraday discussions, 2019. **217**: p. 414-433.
29. Molina, E.R., et al., *A combined theoretical and experimental study of small anthracene–water clusters.* Physical Chemistry Chemical Physics, 2022.
30. Hirunsit, P. and P.B. Balbuena, *Effects of confinement on small water clusters structure and proton transport.* The Journal of Physical Chemistry A, 2007. **111**(42): p. 10722-10731.
31. Mardirossian, N. and M. Head-Gordon, *[small omega]B97X-V: A 10-parameter, range-separated hybrid, generalized gradient approximation density functional with nonlocal correlation, designed by a survival-of-the-fittest strategy.* Physical Chemistry Chemical Physics, 2014. **16**(21): p. 9904-9924.

32. Dunning , T.H., Jr, *Gaussian basis sets for use in correlated molecular calculations. I. The atoms boron through neon and hydrogen.* The Journal of Chemical Physics, 1989. **90**(2): p. 1007-1023.
33. Kendall, R.A., T.H.D. Jr., and R.J. Harrison, *Electron affinities of the first-row atoms revisited. Systematic basis sets and wave functions.* The Journal of Chemical Physics, 1992. **96**(9): p. 6796-6806.
34. Shao, Y., et al., *Advances in molecular quantum chemistry contained in the Q-Chem 4 program package.* Molecular Physics, 2015. **113**(2): p. 184-215.
35. Zhang, B., et al., *Infrared Spectroscopy of Neutral Water Dimer Based on a Tunable Vacuum Ultraviolet Free Electron Laser.* The Journal of Physical Chemistry Letters, 2020. **11**(3): p. 851-855.
36. Zhang, B., et al., *Infrared spectroscopy of neutral water clusters at finite temperature: Evidence for a noncyclic pentamer.* Proceedings of the National Academy of Sciences, 2020. **117**(27): p. 15423-15428.
37. Li, G., et al., *Infrared spectroscopic study of hydrogen bonding topologies in the smallest ice cube.* Nature Communications, 2020. **11**(1): p. 5449.
38. Chakraborty, S., A.D. Stubbs, and T.F. Kahan, *Direct Observation of Anthracene Clusters at Ice Surfaces.* Journal of the American Chemical Society, 2022. **144**(2): p. 751-756.
39. Das, A., et al., *Dynamics of Anthracene Excimer Formation within a Water-Soluble Nanocavity at Room Temperature.* Journal of the American Chemical Society, 2021. **143**(4): p. 2025-2036.